

CONTROLLING GALLING IN SHEET METAL FORMING OF HIGH STRENGTH STEELS: A NUMERICAL APPROACH

Edwin Gelinck – TNO, Eindhoven, The Netherlands
Emile van der Heide – TNO, Eindhoven, The Netherlands
Matthijn de Rooij – University of Twente, Enschede, The Netherlands
Dik Schipper – University of Twente, Enschede, The Netherlands

ABSTRACT

In many forming processes galling is a wear process that limits production velocity and formability of parts. Galling limits the lifetime of tools and the quality of the products is affected. For high strength steels problems with galling are of major interest, since forming pressures are high, as well as shear stresses.

In this paper a numerical model is presented, which describes the initiation of galling and follows the growth of the galling lumps. Flash temperatures are calculated and compared to the critical temperature of the boundary layer at the interface of the sheet and individual tool summits. In case galling occurs at an interface, lump growth can be calculated, as well as the rate of lump growth. In some cases lump growth can cease.

KEYWORDS

Galling, forming, numerical model, lump growth, lubricant failure

INTRODUCTION

High strength steels are subjected to high pressures and high shear stresses in forming processes. In order to study the influence of the different material properties of the tool and sheet material and the operational conditions on the tendency of galling a numerical approach is chosen. Experiments on laboratory scale and on field scale are costly and time consuming. The numerical model presented in this paper is one of the instruments for designing tools for the forming of high strength steels.

The model is based on the models developed by Van der Heide [1] for galling initiation and by De Rooij [2] for lump growth. These models have been combined into one model in which the galling initiation stage is coupled with the lump growth stage.

1. MODEL

The model is based on the models developed by Van der Heide [1] for galling initiation and by De Rooij [2] for lump growth. These models have been combined into one model in which the galling initiation stage is coupled with the lump growth stage. Both models are based on the wear mode map based on the work of Hokkirigawa & Kato [3]. This wear mode map describes the three wear modes of a tool asperity in contact with sheet material:

- *Cutting mode (c)*: material is removed from the soft surface in the form of long ribbon-like chips;
- *Wedge formation (w)*: a wedge of material flows in front of the summit;

- *Ploughing mode (pl)*: material of the soft surface is displaced to the ridges of the wear track and no material is removed from the surface.

In Fig. 1 an asperity in contact with sheet material is shown. The asperity has a radius β , normal force F_n , slides with a velocity v and has a projected contact radius a_s . In Fig. 2 the wear mode diagram is plotted. In the wear mode diagram the transition between the different wear modes are plotted. The attack angle θ (Fig. 1) is shown on the vertical axis and the dimensionless shear strength f_{HK} on the horizontal axis. The dimensionless shear strength f_{HK} is the quotient of the interfacial shear stress and the shear strength of the soft material (the blank of high strength steel).

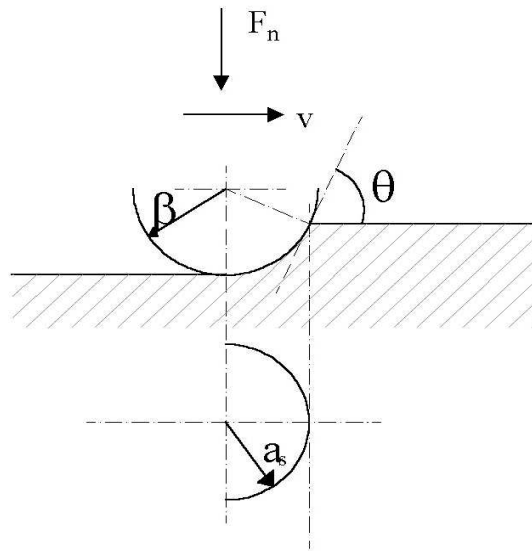


Fig. 1 Tool summit – sheet contact

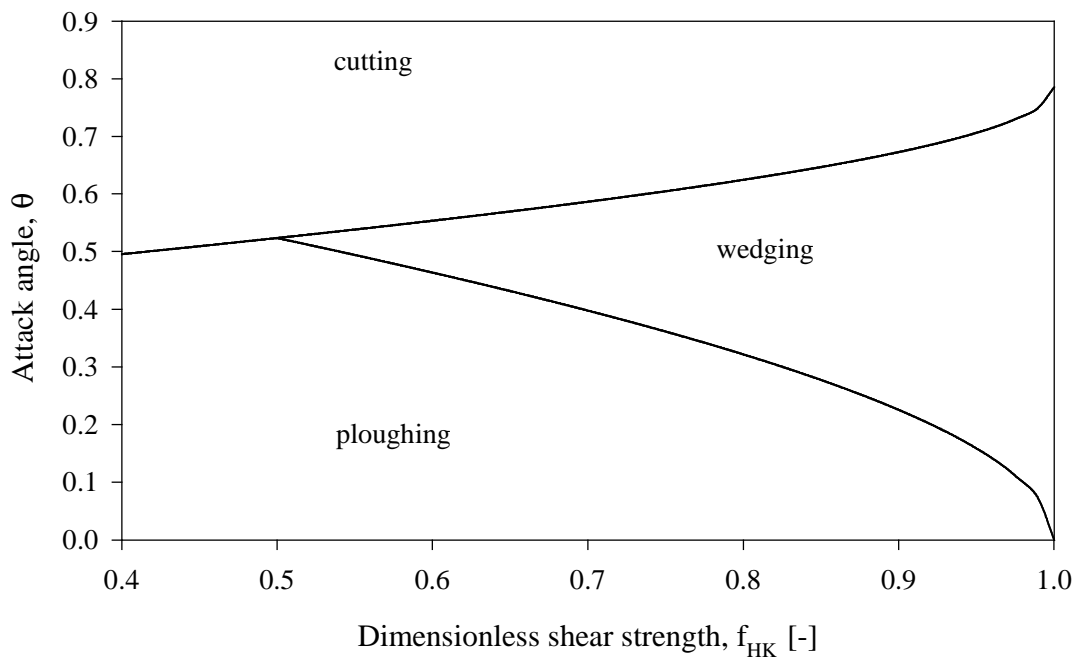


Fig. 2 Wear mode diagram

Asperities in the wedge mode have the potential to initiate or maintain material transfer. However, when lubricant is applied, the local surface temperature T_f also should exceed the critical temperature T_{cr} of the lubricant to be galling. The lubricant breaks down at the specific asperity.

The failure criterion is therefore defined as: $T_f > T_{cr}$ and the contact operates in wedge formation mode after removal of boundary layers.

For **lubricated** contact f_{HK} is between 0.4 and 0.7. In this paper $f_{HK1} = 0.6$ is used for the lubricated contacts. This f_{HK} is denominated also as f_{HK1} . For **unlubricated** contacts f_{HK} is globally between 0.9 and 0.99. In this paper $f_{HK2} = 0.9$ is used for the unlubricated contact. An unlubricated contact is a contact without lubricant (dry), but also a contact with a failing lubricant: $T_f > T_{cr}$.

2. CALCULATIONS

The iteration procedure for calculations is as follows:

1. The roughness of the tool is measured. Asperity heights and asperity curvatures are calculated from the roughness measurement. The starting values and input are determined. The input values for the reference case are listed in Table 1.
2. For each step the value of the separation is calculated. In this step the value for the real area of contact is kept constant.
3. Using the separation of the surfaces the attack angle θ per asperity is calculated.
4. The flash temperature per asperity can be calculated using the theory of Bos and Moes [4], which is based on the theory of Carslaw and Jeager [5]. For this purpose the coefficient of friction of the appropriate regime in the wear mode map is calculated. Using the thermal conductivity values of the tool and sheet the heat transfer from the contact can be calculated and thus using the specific heat of the sheet the local temperature can be calculated. These calculations are performed for the lubricated contact situation. In case the contact is lubricated the f_{HK1} value is between 0.4 and 0.7. In the present case $f_{HK1} = 0.6$ is taken.
5. For all asperities in which the flash temperature exceeds the critical temperature are virtually unlubricated. At all other asperities no galling can occur.
6. For all asperities that can potentially be galling ($T_f > T_{cr}$) the value of f_{HK} is set to 0.9, since this is the value of f_{HK} for unlubricated contacts. It is then checked whether at $f_{HK} = 0.9$ the asperity is in the wedge regime. If not in the wedge regime no galling on that asperity. In case the asperity is in the wedge regime galling occurs at that asperity.
7. In case galling occurs on an asperity the summit rise Δs is calculated for that asperity.
8. Finally the new separation and attack angles per asperity are calculated keeping the real area of contact constant at each iteration step.
9. Return to number 4.
10. In case no asperity is galling (anymore) the iteration is stopped.

The complete mathematics is given below.

Input: roughness

The input in the program is a measured roughness and the load on the contact. The surface of the tool is measured in 3D. The roughness measurement is used to determine which measured points on the surface are summits and the radius of each summit. This can be done in accordance with an often used 8-points criterion in which a point is a summit when it is higher than its eight surrounding points.

Calculation: fraction of contact area, separation

It is assumed that the load, F_N , on the contact is constant. This constraint is equivalent to the demand, that α^* , the fraction of area in contact, should remain constant. The normal load is:

$$F_N = 2\pi H A_{nom} \eta \sum_i \beta_i \cdot (s_i - h) \quad (1)$$

With H hardness, A_{nom} nominal area and η summit density, β_i summit radius per summit, s_i summit height and h the separation between the contacting surfaces.

Or in term of α^* :

$$\alpha^* = 2\pi \eta \sum_i \beta_i \cdot (s_i - h) \quad (2)$$

By assuming a normal load, the separation h can be calculated using a root-finding procedure.

Calculation: attack angle

The attack angles θ per summit (Fig. 1) are calculated according to:

$$\theta = \begin{cases} \arctan\left(\frac{\sqrt{(s-h) \cdot (2\beta + h - s)}}{\beta + h - s}\right) & \text{if } s-h < \beta \\ \frac{\pi}{2} & \text{otherwise} \end{cases} \quad (3)$$

Calculation: flash temperature

Calculation of the flash temperature is done in more steps. The flash temperature is calculated per individual summit.

First the coefficient of friction is calculated. This coefficient of friction depends on the wear mode of the specific summit. The transitions can not only be depicted in a wear mode diagram, but are also available as a mathematical expression:

$$\theta_{w,pl \rightarrow c} = 0.25(\pi - \arccos f_{HK}) \quad (4)$$

and

$$\theta_{pl \rightarrow w} = 0.5 \arccos f_{HK} \quad (5)$$

The coefficients of friction in each wear regime:

$$f_c = \tan\left(\theta - \frac{\pi}{4} + \frac{1}{2} \arccos f_{HK}\right) \quad (6)$$

$$f_w = \frac{\left(1 - 2 \sin \xi_1 + \sqrt{1 - f_{HK}^2}\right) \cdot \sin \theta + f_{HK} \cos \theta}{\left(1 - 2 \sin \xi_1 + \sqrt{1 - f_{HK}^2}\right) \cdot \cos \theta - f_{HK} \sin \theta} \quad (7)$$

$$f_{pl} = \frac{\xi_2 \sin \theta + \cos(\arccos f_{HK} - \theta)}{\xi_2 \cos \theta + \sin(\arccos f_{HK} - \theta)} \quad (8)$$

with:

$$\xi_1 = \theta - \frac{\pi}{4} - \frac{1}{2} \arccos f_{HK} + \arcsin \left(\frac{\sin \theta}{\sqrt{1 - f_{HK}}} \right) \quad (9)$$

and

$$\xi_2 = 1 + \frac{\pi}{2} + \arccos f_{HK} - 2\theta - 2 \arcsin \left(\frac{\sin \theta}{\sqrt{1 - f_{HK}}} \right) \quad (10)$$

In order to calculate the flash temperatures, the effective conductivity K_{eff} is needed as well:

$$K_{eff} = 2.746 \cdot K_{tool} + K_{sheet} \left(10.379 + 7.603 \left(\frac{a \cdot v}{K_{sheet}} \right)^{1.158} \right)^{0.432} \quad (11)$$

with

$$K_{sheet} = \frac{K_{sheet}}{\rho_{sheet} c_{p,sheet}} \quad (12)$$

and

$$a = \frac{1}{2} \beta \sin \theta \quad (13)$$

The load per summit is:

$$F_n = \frac{1}{2} \pi a^2 H_{sheet} \quad (14)$$

The flash temperature per summit can now be calculated:

$$T_f = \frac{f \cdot F_n \cdot v}{a \cdot K_{eff}} \quad (15)$$

For f the appropriate coefficient of friction from the wear regime applicable for the specific summit should be used (Eqs. 6, 7 and 8).

Check: summit lubricated or not lubricated

The value for f_{HK} applied in the temperature calculations is the f_{HK} at lubricated conditions ($f_{HK1} = 0.6$, or between 0.4 and 0.7), since the contacts of the summits are considered to be lubricated, unless the flash temperature exceeds the critical temperature of the lubricant. If the flash temperature at a summit exceeds the critical temperature a contact fails and the contact is considered to be virtually unlubricated.

Check: summit galling or not galling

In the case the flash temperature on a summit exceeds the critical temperature, it has to be checked whether the summit is in the wedge regime. Since the summit is virtually unlubricated (lubricant failed) the high f_{HK} value is used for unlubricated contacts, e.g. $f_{HK2} = 0.9$. The boundaries of the wedge regime are again given in eq. 4 and 5 (with $f_{HK2} = 0.9$).

Summits that exceed the critical temperature and are in the wedging regime are galling and for those summits the increase in height has to be calculated.

Calculation: height increase of galling summits

The increase in height Δs of a galling summit is given by [2] as:

$$\Delta s = \begin{cases} m_2 6\sqrt{3}\pi H (s-h)^2 Q & \text{if } H^2 < \frac{2\Delta\gamma E^*}{\pi\sqrt{2\beta}(s-h)} \\ m_2 6\sqrt{6} \frac{\Delta\gamma E^*}{H} \frac{(s-h)^{3/2}}{\sqrt{\beta}} Q & \text{if } H^2 \geq \frac{2\Delta\gamma E^*}{\pi\sqrt{2\beta}(s-h)} \end{cases} \quad (16)$$

with

$$Q = \frac{\sin^2 \theta + \frac{1}{2} \sin 2\theta}{1 + \sin 2\theta} \quad (17)$$

and $\Delta\gamma$ the specific adhesion energy and E^* the reduced elastic modulus.

The value of m_2 is given by [2] as constant in the galling model (unit: N^{-1}). The value for m_2 given by [2]: $m_2 = 2 \cdot 10^{-4} N^{-1}$. This value is valid for non-coated steels.

This increase Δs is added to the current height of the summit to obtain the new summit height, and thus a new summit height distribution. This new summit height distribution is used for the next pass.

3. Results

Using the parameters of Table 1 calculations have been performed. Various parameters can be studied in this process, e.g. the number of asperities that is galling per summit, the growth per asperity, the attack angle vs. height of an asperity and the temperature per asperity. These parameters can all be followed when being calculated. Each summit has its own attack angle, flash temperature and increase in height at each pass. A cloud of points, which develops per pass (iteration), can therefore be followed. An example of the representation of points is given in Figs. 3 to 6. In these figures the cloud of points is given at a single pass. In the current case pass number 100.

Fig. 3 gives the attack angles of the individual summits as function of the height. At the beginning of each cycle the attack angles have to be recalculated, since the reference height (h_0) of the surface has changed. Therefore the attack angles of the summits that have not been galling in the last iteration decrease slightly, whilst the attack angles of the summits that have been galling in the last iteration will increase, eq. (3)). The summits that have been galling will go deeper into the sheet material, caused by the increase in height. These summits are denoted in the figures as the galling summits.

In Fig. 4 the flash temperatures that have been calculated are depicted as function of the attack angle of the summit. In this figure the role of the wear mode diagram (Fig. 2) can be clearly seen. In the cutting regime the flash temperatures are relatively low. This explains the drop in the temperatures above the attack angle $\theta_1(f_{HK1})$, i.e. at the transition from wedging to cutting in the lubricated case (vertical line in Fig. 4). Above the critical temperature of 60 °C the lubricant fails, and thus these summits are virtually unlubricated. A few summits which are in the cutting mode when lubricated ($f_{HK1} = 0.6$) do reach a temperature above the critical temperature of the lubricant. Since the wedge

regime diverges for increasing values of f_{HK} , some of these summits are in the wedge regime at $f_{HK2} = 0.9$, combined with the fact that these summits are virtually unlubricated, results in galling of these summits as well.

Table 1 Parameters used in reference case

Quantity	Symbol	Value	Unit
<i>Tool properties WN 1.2379</i>			
Thermal conductivity tool	K_t	20	$W m^{-1} K^{-1}$
<i>Sheet properties 1400 M cold rolled</i>			
Thermal conductivity sheet	K_s	64	$W m^{-1} K^{-1}$
Density	ρ	8000	$kg m^{-3}$
Specific heat	c_p	460	$J kg^{-1} K^{-1}$
Hardness	H	1.8	GPa
Temperature sheet	T_s	20	$^{\circ}C$
<i>Combined properties</i>			
Reduced elastic modulus	E^*	69	GPa
Specific adhesion energy	$\Delta\gamma$	2.5	$N m^{-1}$
Constant in galling model	m_2	$2 \cdot 10^{-4}$	N^{-1}
Dimensionless shear strength	f_{HK1} (lubricated)	0.6	-
	f_{HK2} (unlubricated)	0.9	-
<i>Lubricant property</i>			
Critical Temperature	T_{cr}	60	$^{\circ}C$
<i>Operational conditions</i>			
Velocity	v	1.0	$m s^{-1}$
Starting value h_0	$h_{0,start}$	-2σ	m

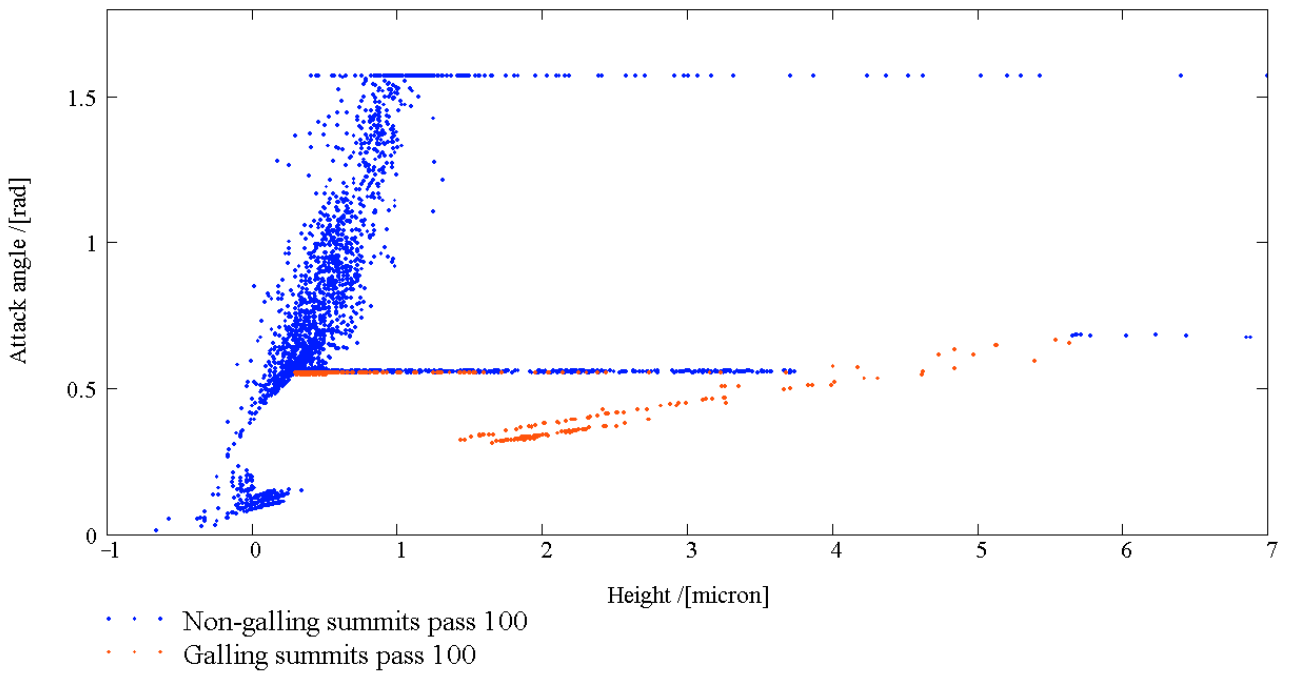


Fig. 3 Attack angle vs. height at pass 100

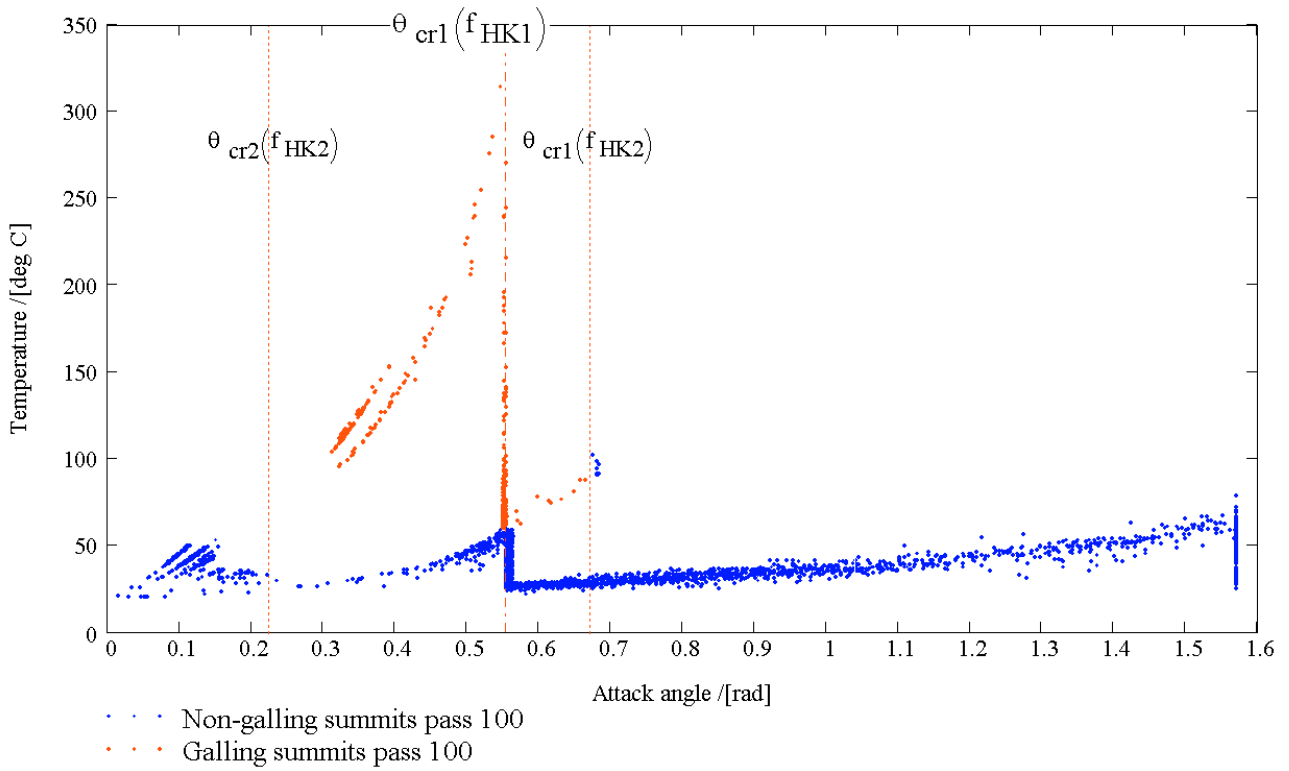


Fig. 4 Temperature of summits vs. attack angle at pass 100

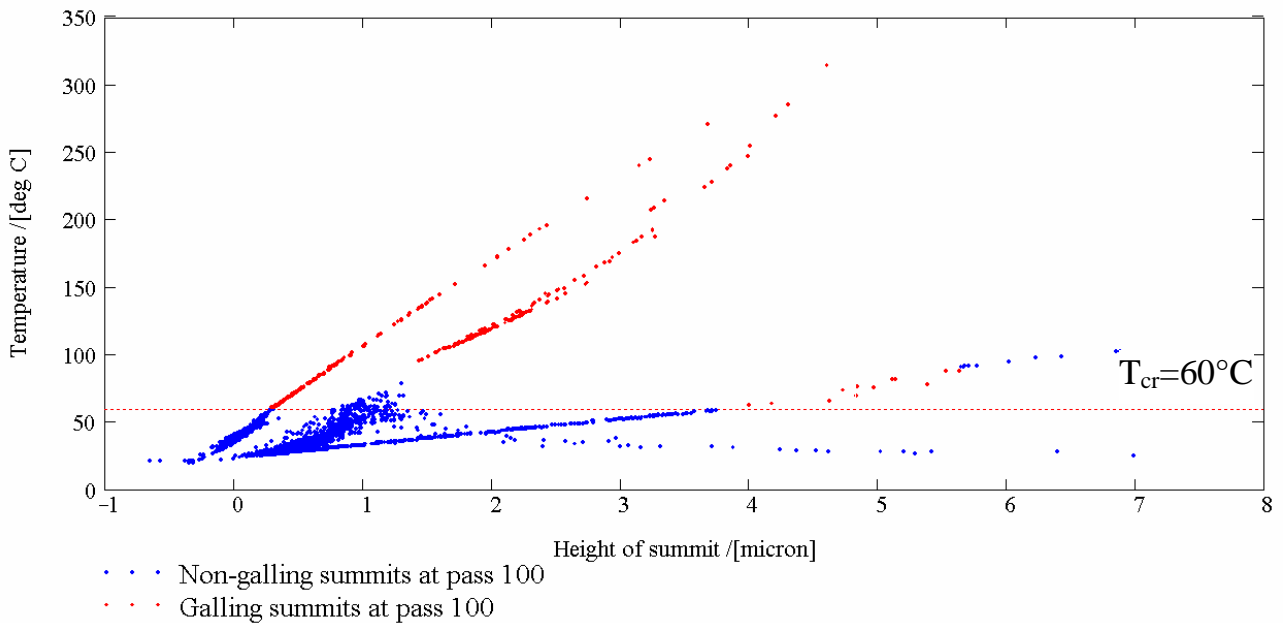


Fig. 5 Temperature of summits vs. summit height at pass 100

The flash temperatures of the summits are plotted against the summit height in Fig. 5. In this figure the critical temperature $T_{cr} = 60^{\circ}\text{C}$ is indicated. It shows that not all summits that exceed the critical temperature gall. In Fig. 3 it can be seen that most of these summits are in the cutting regime and some in the ploughing regime.

At the end of each iteration the change in height is calculated for each of the summits that is galling. In Fig. 6 the change in height of all summits is given as function of the height of the summit. Of course the summits which are galling have a non-zero change in height. The figure shows that the higher summits that gall have a larger change in height.

Because of the larger change in height, the attack angle will increase subsequently and most of these summits will not gall in one of the subsequent passes. Other summits that do not gall in the current pass can gall in one of the subsequent passes. The attack angle of these summits decreases in the current pass, and their attack angle can cross the critical attack angle of cutting or wedging in the wear mode diagram. Then this summit is in the wedge regime at the next pass.

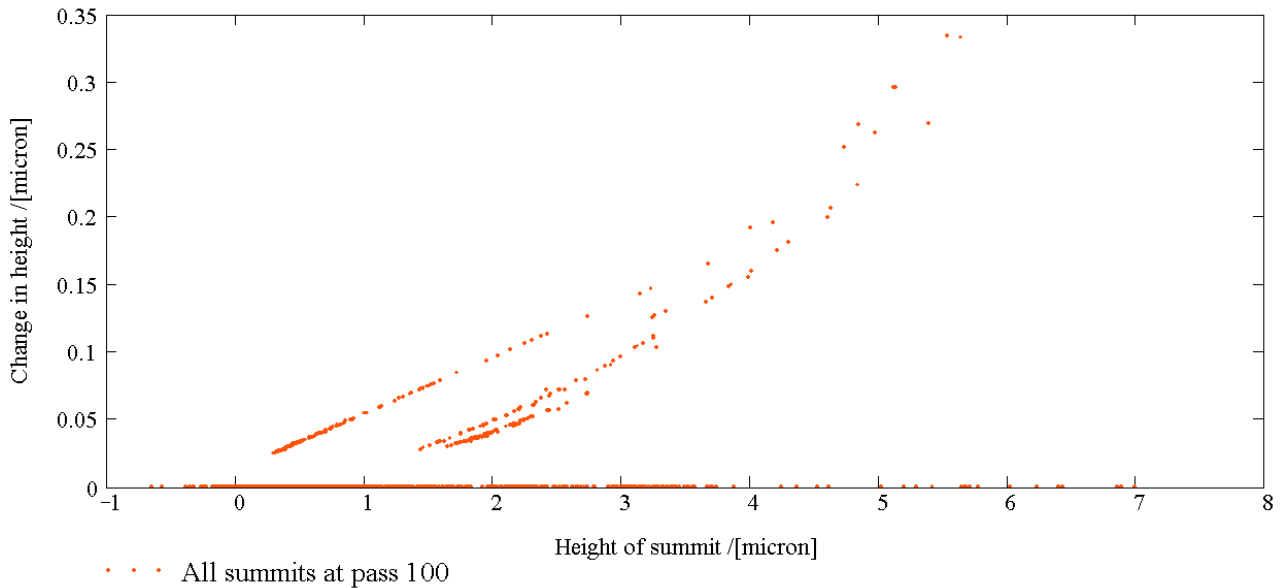


Fig. 6 Change in height of summits vs. summit height at pass 100

Over the subsequent passes high summits (lumps) will arise, which will cause deep scratches. In the forming process the depth of the scratches left behind on the product is the most interesting criterion for approval of a product. In case a scratch is too deep the scratch can not be masked with lacquer. A criterion used in the industry is a maximum depth of the scratch of 10 μm . Deeper scratches lead to rejection of the product. The depth of the scratch is therefore used as criterion in this paper as well.

In Fig. 7 the calculated separation is plotted against the pass number. The program calculates the lump growth on the tool. The lumps on the tool cause scratches in the sheet material. These scratches will be just as deep, as the lump is high. As criterion for the lump growth the change in height of the highest asperity has been chosen.

There are two possible criteria for the lump height. The first is the change in height of the highest asperity. The second is the change in the value for the separation. In this paper the latter had been chosen, since the height of the highest asperity is a more subject to statistical noise.

The depth of the scratch is equal to the increase in the separation, since the lump growth is equal to the change in separation. The separation starts at $h_0 = -0.88 \mu\text{m}$ and therefore the end criterion for disapproval for a product is $h_0 = 9.12 \mu\text{m}$. This value is reached after 228 passes for the reference case in Table 1. This number of passes is related to the tool life, the number of products that can be made with the tool.

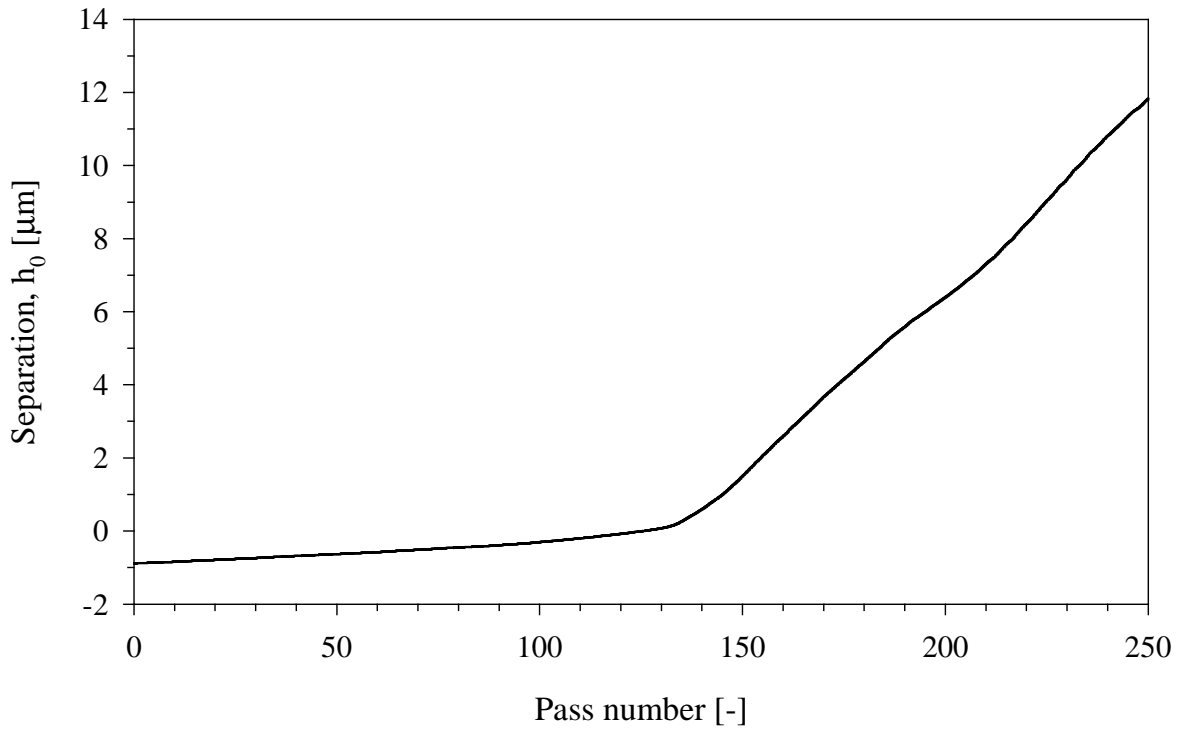


Fig. 7 Separation or lump growth for the reference case ($h_0 = -2\sigma$)

In cases the load is less severe the starting value of h_0 will be higher. In Fig. 8 it is shown, that galling can stop after a limited number of cycles (this case 67), and that the depth of the scratch that is made with the tool is only very small, less than $0.01 \mu\text{m}$ for this case. The case shown in Fig. 8 will therefore not lead to rejection of the product.

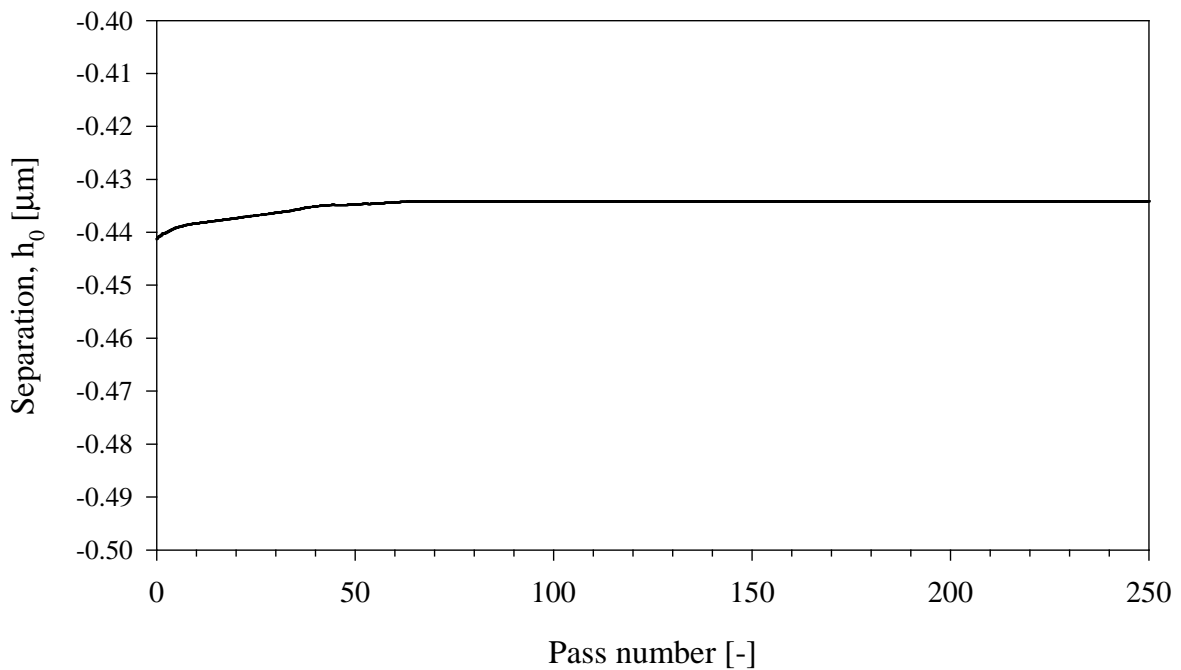


Fig. 8 Separation or lump growth for $h_0 = -\sigma$.

4. Conclusions

A mathematical model has been presented, which combines galling initiation and lump growth in forming processes. This model has been applied to the forming process of super high strength steel. The model can be used to predict whether galling in deep drawing will occur and at which rate it will take place. Action can be taken to decrease the probability of galling. The model can be applied as an instrument to predict the lifetime of the tool used in the forming process.

An interesting result of the calculations shown is that the galling process can stop under certain conditions. The height of the highest summit is only slightly above its starting value, and thus it can be said that in that case no scoring has occurred. The products will not be rejected.

A parameter study of the most important parameters is foreseen.

Experimental validation of both the initiation model and the lump growth model has been performed. Currently measurements are performed on super high strength steels as well.

REFERENCES

- 1) E. van der Heide and D.J. Schipper, On the frictional heating in single summit contacts: towards failure at asperity level in lubricated systems, *Journal of Tribology*, 126 (2). (2004), p.275.
- 2) M.B. de Rooij, Tribological aspects of unlubricated deep drawing processes, PhD Thesis, University of Twente (1998).
- 3) K. Hokkirigawa and K. Kato, An experimental and theoretical investigation of ploughing, cutting and wedge formation during abrasive wear, *Tribology International*, 21 (1), (1988) p. 51.
- 4) J. Bos and H. Moes, Frictional heating of tribological contacts, *Journal of Tribology*, 117, (1995), p. 171
- 5) H.S. Carslaw and J.C. Jaeger, *Conduction of heat in solids*, Oxford University Press, Oxford (1959).